



Publication Year	2018
Acceptance in OA@INAF	2020-10-28T17:07:31Z
Title	MAORY real-time computer preliminary design
Authors	FOPPIANI, ITALO; SCHREIBER, LAURA; AGAPITO, GUIDO; ARCIDIACONO, CARMELO; BARUFFOLO, Andrea; et al.
DOI	10.1117/12.2311618
Handle	http://hdl.handle.net/20.500.12386/28050
Series	PROCEEDINGS OF SPIE
Number	10703

PROCEEDINGS OF SPIE

[SPIDigitalLibrary.org/conference-proceedings-of-spie](https://spiedigitallibrary.org/conference-proceedings-of-spie)

MAORY real-time computer preliminary design

Foppiani, Italo, Schreiber, Laura, Agapito, Guido, Arcidiacono, Carmelo, Baruffolo, Andrea, et al.

Italo Foppiani, Laura Schreiber, Guido Agapito, Carmelo Arcidiacono, Andrea Baruffolo, Giovanni Bregoli, Lorenzo Busoni, Enrico Cascone, Giuseppe Cosentino, Michele Bellazzini, Paolo Ciliegi, Emiliano Diolaiti, Simone Esposito, Philippe Feautrier, Roberto Ragazzoni, "MAORY real-time computer preliminary design," Proc. SPIE 10703, Adaptive Optics Systems VI, 1070343 (18 July 2018); doi: 10.1117/12.2311618

SPIE.

Event: SPIE Astronomical Telescopes + Instrumentation, 2018, Austin, Texas, United States

MAORY Real Time Computer Preliminary Design

Italo Foppiani^a, Laura Schreiber^a, Guido Agapito^b, Carmelo Arcidiacono^a, Andrea Baruffolo^c, Giovanni Bregoli^a, Lorenzo Busoni^b, Enrico Cascone^d, Giuseppe Cosentino^e, Michele Bellazzini^a, Paolo Ciliegi^a, Emiliano Diolaiti^a, Simone Esposito^b, Philippe Feautrier^f, Roberto Ragazzoni^c

^aINAF - Osservatorio di Astrofisica e Scienza dello Spazio di Bologna, via Gobetti 93/3, 40129 Bologna, Italy;

^bINAF - Osservatorio Astrofisico di Arcetri, largo E. Fermi 5, 50125 Firenze, Italy;

^cINAF - Osservatorio Astronomico di Padova, vicolo dell'Osservatorio 5, 35122 Padova, Italy;

^dINAF - Osservatorio Astronomico di Capodimonte, salita Moiariello 16, 80131, Napoli, Italy;

^eAlma Mater Studiorum, Università di Bologna, DIFA Dipartimento di Fisica e Astronomia, via Gobetti 93/2, 40129 Bologna, Italy;

^fUniversité Joseph Fourier-Grenoble 1/CNRS-INSU, IPAG Institut de Planétologie et d'Astrophysique de Grenoble UMR 5274, 38041 Grenoble, France

ABSTRACT

MAORY is the Multi-conjugate Adaptive Optics module for the Extremely Large Telescope and it will be located on the Nasmyth platform of the telescope to feed scientific instruments. MAORY will re-image the telescope focal plane providing multi-conjugate adaptive optics correction of the wavefront distortion induced by the atmosphere. The system is based on six laser guide stars and three natural guide stars for sensing the wavefront distortion and three deformable mirrors for correcting it. We will show the current status of the preliminary design of the Real Time Computer in charge of carrying out all the calculations based on the measurements of the guide stars wavefront sensors. The hard real time (primary) loops are in charge of controlling the deformable mirrors and the lasers jitter compensation while the soft real-time (secondary) loops are in charge of updating the primary loops parameters as well as measuring or estimating the atmospheric parameters and the system performance. Telemetry data management/recording and calibration are the other tasks carried out by the real time computer.

Keywords: Multi-Conjugate Adaptive Optics, Extremely Large Telescope, MAORY, Real Time Computer, Control

1. INTRODUCTION

MAORY^[1] is the Multi-conjugate Adaptive Optics Relay for the Extremely Large Telescope (ELT)^[2] first Light. It will provide two ports to feed scientific instruments: a vertical port and a gravity invariant one. The latter is specifically designed for the Multi-Adaptive Optics Imaging Camera for Deep Observations (MICADO)^[3] for which an un-vignetted and corrected Field of View (FoV) of about 1 arcminute is required.

Two adaptive optics modes are foreseen to support the MICADO near-infrared camera: Multi-Conjugate Adaptive Optics (MCAO) and Single-Conjugate Adaptive Optics (SCAO)^[4]. In the MCAO mode, MAORY uses the adaptive mirror M4 and tip-tilt mirror M5 in the telescope and up to two post-focal adaptive mirrors (DM1 and DM2) to achieve high performance with excellent uniformity of the point spread function (PSF) across the scientific FoV; in order to ensure high sky coverage, wavefront sensing is based on up to six Laser Guide Stars (LGS) projected from the telescope side in a constellation of 1.5 or 2 arcminutes angular diameter. While the LGS WFSs^[5] measure the high order (HO) wavefront distortions, three natural guide stars (NGS) WFSs measure the low order ones. Each NGS WFS^[6] sensor is equipped with a double channel: the low order (LO) sensors measures in real time the wavefront tip-tilt, focus and astigmatism in H band while the reference (REF) sensors measure at slower rate the wavefront distortions of low to medium order in R+I band. The three NGS are positioned over a 3 arcmin technical FoV.

2. MAORY CONTROL OVERVIEW

Figure 1 shows the MAORY MCAO functional block diagram. The light from the adaptive telescope (dashed box on the top of the Figure) enters MAORY through the Main Path Optics (Common path). Upon wavefront compensation by the Post-focal DMs (which complement the telescope's M4/M5), indicated in the figure as INS-DM1/DM2, the light is split by a dichroic beam-splitter: the light of wavelength shorter than about 600 nm is propagated from the dichroic beam-splitter through the LGS Path Optics and then to the LGS WFS sub-system.

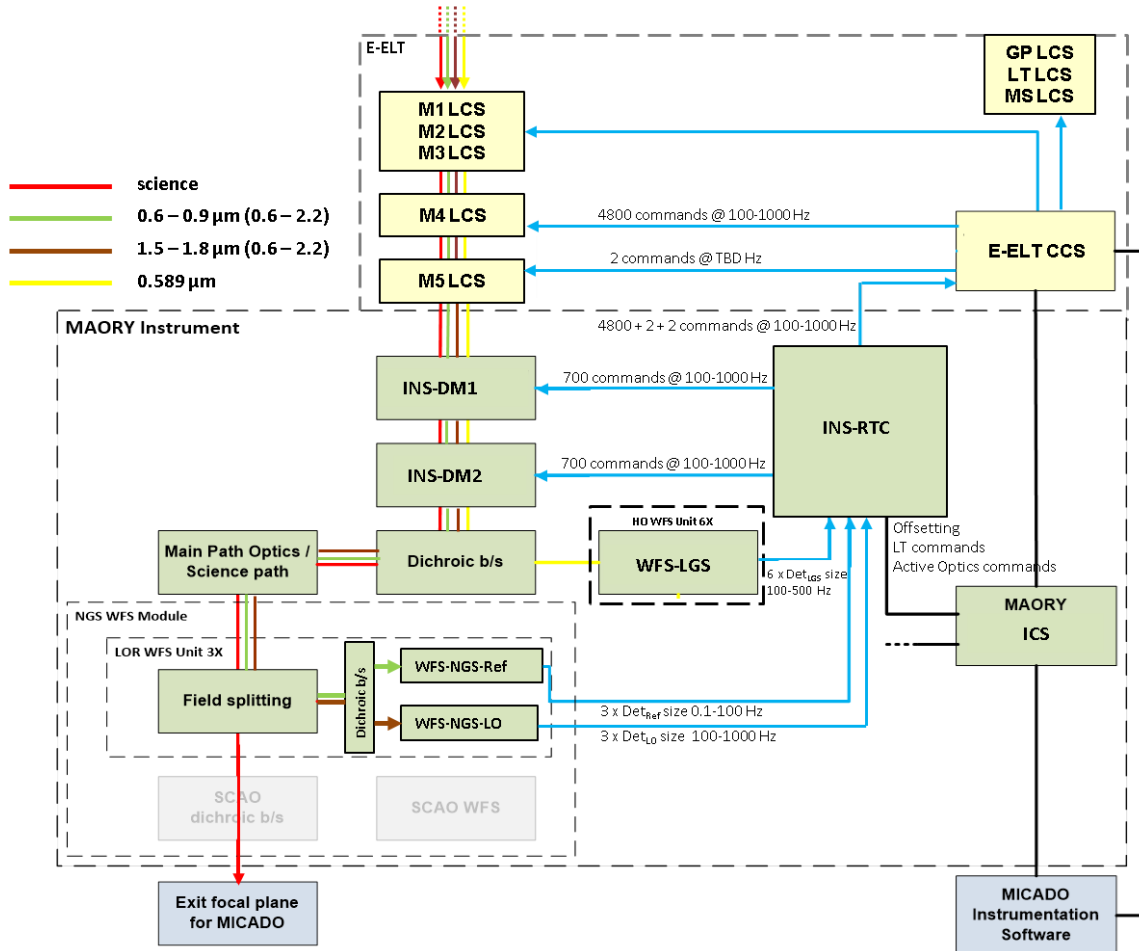


Figure 1. MAORY AO overview (MCAO configuration). Red lines: science light path. Yellow lines: LGS light path. Green lines: NGS visible light path. Brown lines: NGS infrared light path. Blue lines: real-time signals. Black lines: non real-time signals. Blocks in light grey are not used in MCAO mode. Those devices inside the E-ELT dashed box (yellow boxes) do not belong to the MAORY AO subsystem but are part of the E-ELT infrastructure. DetLGS, DetLO and DetRef size stand respectively for the size of the individual WFS-LGS, WFS-NGS-LO and WFS-NGS-Ref detectors

The light of wavelength longer than 600 nm is reflected in the direction of the Science path to the gravity invariant Exit Port. The MAORY exit focal plane is made then available to MICADO. The light of the required NGSs is picked off by the WFS Units (LO + REF = LOR WFSs) in the NGS WFS Module and it is divided in wavelength by a dichroic beam-splitter. It is under evaluation the possibility to insert devoted DMs in front of the NGS WFS to correct the wavefront in the direction of the NGS only and improve the star image quality on the detector. This technique is called Dual Adaptive Optics^[7] and it would permit to improve the sky coverage. In this paper we will not enter in details of this technique. We will mention it only in the context of system dimensioning and actuator description.

The wavefront measurements performed by the LGS and LOR WFSs in the MCAO mode are collected by the MAORY RTC, which drives in closed loop the MAORY Post-focal DMs, dual AO DMs (in case this technique is adopted) and,

passing through the CCS, the actuators in the telescope, including the adaptive quaternary mirror M4, the tip-tilt mirror M5 and the Laser launching facility. This facility provides a fast Jitter Mirror to compensate for the fast tip-tilt due to the Laser jitter. This jitter mirror could be used also to introduce a known periodic tilt signal on both axes to produce a known sub-pixel shift in the LGS image. This signal is required to support centroid gain calibration procedures which should be performed during operations to mitigate WFS non-linearity and other effects that can arise when working in under-sampled conditions.

3. MAORY REAL TIME SENSORS AND ACTUATORS

As already mentioned, MAORY wavefront sensing relies on six LGS WFSs, three LO WFS and three REF WFS and two post-focal DMs, together with telescope M4 and M5, are responsible for the wavefront correction. Table 1 summarizes the MAORY system baseline driving the RTC specifications. As previously said, we are evaluating the possibility to implement small local DMs at the level of the NGS WFS in order to improve the sky coverage. These actuators are not considered in the table. Many trade-offs are still under investigation, and for simplicity we report only the actual baseline parameters.

Table 1. MAORY system baseline

MAORY RT SENSORS	LGS WFS	Number	6
		Wavelength	0.589 μm
		Type	Shack-Hartmann
		Geometry	80 X 80 sub-apertures
		Detector type ^[8]	CMOS
		Detector size ^[8]	800 X 800
		Frame rate ^[8]	500 Hz
	Readout mode ^[8]	Rolling shutter	
	NGS LO WFS	Number	3
		Wavelength	1.5 μm – 1.8 μm
		Type	Shack-Hartmann
		Geometry	2 X 2 sub-apertures
		Detector type ^[8]	HgCdTe APD
		Detector size ^[8]	320 X 256
		Frame rate ^[8]	100 Hz – 1000 Hz
	Readout mode ^[8]	CDS or Fowler Sampling	
	NGS REF WFS	Number	3
		Wavelength	0.6 μm – 1.1 μm
		Type	Shack-Hartmann
		Geometry	10 X 10 – 20 X 20 sub-apertures ¹
		Detector type ^[8]	CCD
Detector size ^[8]		240 X 240	
Frame rate ^[8]		0.1 Hz – 100 Hz	
Readout mode ^[8]	Frame Transfer		
MAORY RT ACTUATORS	Telescope M4	Number	1
		Type	Shape control
		Controlled DoF	4800
		Maximum rate	1000 Hz
	Post Focal DMs	Number	2
		Type	Shape control
		Controlled DoF	700
		Maximum rate	1000 Hz

¹ The number of REF WFS sub-apertures is a crucial parameter. From this choice depends the possibility to measure spurious non-atmospheric medium order aberrations by truth sensing. This trade-off is still not concluded.

The LGS WFS sub-aperture FoV is a key parameter that could have an impact on the performance. A larger number of pixels would allow us to have a FoV properly dimensioned to avoid spot truncation at the maximum spot elongation. The truncation of elongated spots could in fact cause the injection of spurious low order modes in the loop and a performance degradation^[9]. Many back-up solutions are under study to mitigate this risk using a small detector. A smaller number of pixels is acceptable, providing that: an auxiliary loop (the REF loop) monitors for low/medium order modes arising from spot truncation effects; the LGS image is under-sampled in order to maximize the available FoV (centroid calibration procedures are then needed). The baseline detector is the NGSD 880X840, but LGS WFS will be probably designed, in terms of volumes allocation, to allow the future implementation of a bigger detector (1600X1600). The RTC shall be also dimensioned taking this future upgrade into account.

4. MAORY REAL TIME CORE CONTROL STRATEGY

The actual MAORY RTC architecture foresees WFS processing tasks that take care of WFS image reconstruction and calibration, centroid calculation and finally provide the slope measurements. The baseline control strategy is based on Pseudo Open-Loop Control (POLC) algorithm. In order to reduce the required computing power, the coordinate system of the modal bases that describe the reconstructed atmospheric layers, the pupil and metapupils wavefronts as well as the DMs commands, is kept fixed with respect to the nominal telescope pupil, i.e. all the planes are kept at constant distance, orientation and centering. The spread of the turbulence strength among the reconstructed layers will thus depend on telescope elevation other than the atmosphere properties. The post focal DMs surfaces result rotating with respect to the coordinates system as consequence of the telescope elevation and the WFS NGS, both LO and REF, result rotating as consequence of sky rotation.

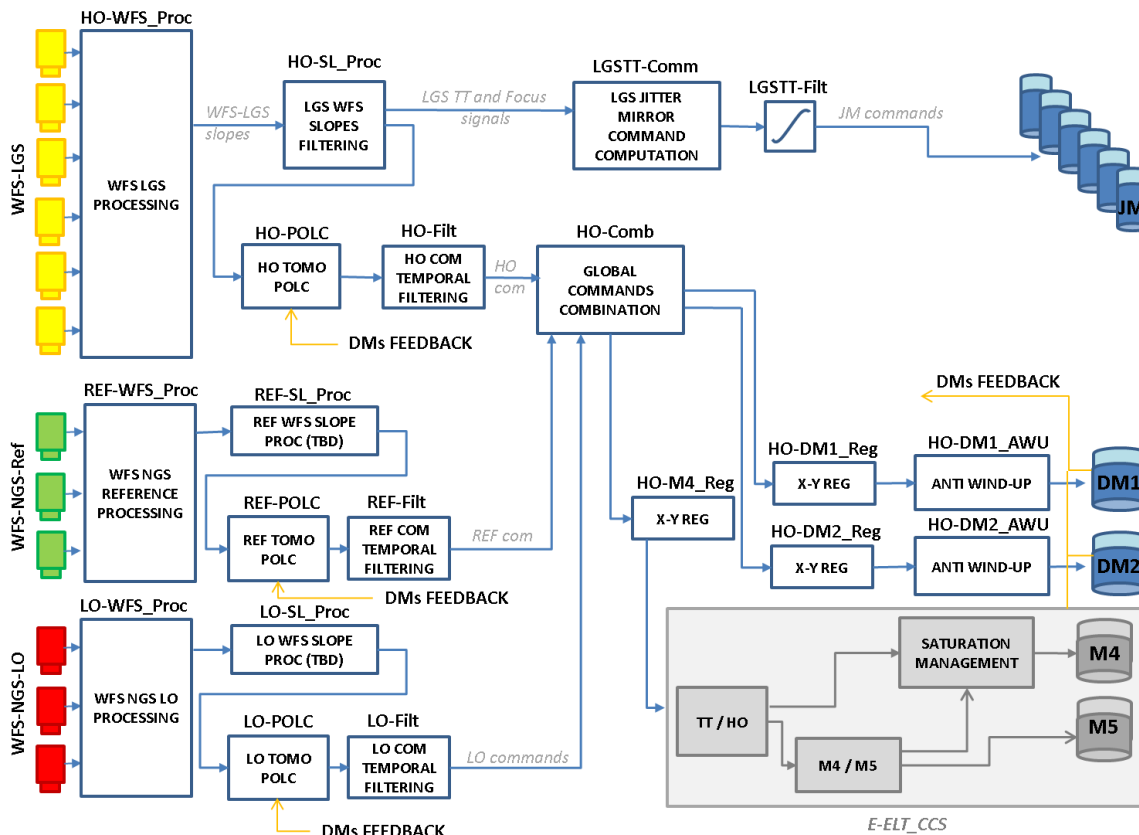


Figure 2. Simplified, overall control loop and tasks diagram for MCAO configuration

The POLC algorithm is implemented in the three control loops HO, REF and LO to compute the high order and the low order modal commands of the DMs as well as the reference offsets. Figure 2 shows a simplified control loop diagram and the main RT tasks briefly described in the following.

4.1 The WFS processing tasks

The real time computer will process the WFS images into slopes for the reconstruction algorithm. After reconstruction and calibration of the image, centroids for each sub-aperture will be computed. Depending on the considered channel and on its peculiarities (LGS, NGS LO or NGS REF), a different centroid algorithm will be implemented. The LGS WFS spots are characterized by a variable shape across the pupil. In fact, due to perspective elongation, some of the spots, the ones located on the opposite side of the pupil with respect to the position of the laser launcher, will be elongated. This elongation impacts the centroid measurements, that is less precise where the image is less compact. For this reason, specific and more complex algorithms are foreseen for the LGS spots centroid computation. The actual baseline is to use the Weighted Center of Gravity algorithm: the spot intensity is weighted through a weighting map. This map can be built by averaging for a certain time interval the WFS images. This map will be optimized in Soft Real Time with a time step of some seconds. Another important Soft Real Time task that could run in parallel will be devoted to the centroid gain optimization, in case the LGS WFS will work in sub-sampled condition. While for the Reference WFS channel a simple center of gravity, probably with a threshold, is considered, in the LO channel the situation could be more complex. In order to reject the IR background, the slopes will be computed on a window (one for each sub-aperture) whose dimensions are configurable parameters and whose positioning is updated on the basis of the running mean of the last images. The slopes will be computed as either the centre of gravity or the correlation with a template.

4.2 The reconstruction and command calculation

The POLC algorithm is implemented in the three primary loops carried out in hard real time of Figure 2: the HO and LO loops compute the real time commands on the basis of LGS and NGS LO measurements while the REF loop, based on NGS REF measurements, corrects slower wavefront distortion of low to medium order poorly sensed/corrected by other loops or even due to them.

Table 2. Dimensioning parameters

	Number of WFS (N_{WFS})	Number of slopes per WFS (N_{WFS})	Number of slopes (N_{SLP})	Number of layers (N_L)	Number of modes per layer (N_{ML})	Number of modes on the pupil (N_{MP})	Number of optimization directions (N_{opt})	Number of commands (N_{com})
HO	6	9600	57600	10	5000	5000	9	6200
LO	3	600	1800	10	200	200	9	300
REF	3	8	24	10	20	20	9	11

In Table 2 are summarized dimensioning parameters. As a baseline the HO and LO tomography and commands are computed in a split way so that the eventual commands are the simple concatenation of the results of the two loops. The REF commands are added as offsets. The DM commands are numerically shifted to compensate for DMs mis-registration and an anti-windup control is foreseen. The latter is supposed to receive feedback from the saturation management performed by DMs control units. The post focal DMs will also carry out numerical rotation of the commands to compensate for the DMs rotation with respect the coordinate system.

The Pseudo Open-Loop (POL) measurements (slopes) are reconstructed from the closed loop measurements and DMs commands and then they are used to directly compute the command. In order to save computing power, the time filtering is applied directly to the commands rather than to the tomographic reconstructed turbulence so that only one matrix vector multiplication is needed. The only required parameter is the control matrix $P_x R_x$, given by the product of the tomographic reconstructor R_x and the fitting projector P_x . The generic subscript x is used instead of h, l or r specific of each HO, LO and REF loop. The matrix R_x reconstructs the tomography of the turbulence from the POL measurement and is the regularized pseudo inverse of $A_x = IP_x ML_x^{GS}$ where IP_x is Interaction matrix that computes the detectors

slopes from the modal descriptions of the pupil wavefront and ML_x^{GS} is the geometric projector that computes the pupil wavefront in all the directions of the guide stars from the atmospheric turbulence profile. The matrix R_x is thus:

$$R_x = \left[(A_x^T CN_x^{-1} A_x + C_\phi^{-1})^{-1} \times (A_x^T CN_x^{-1}) \right]$$

or equivalently

$$R_x = C_\phi A_x^T \left[(A_x C_\phi A_x^T + CN_x) \right]^{-1}$$

where $A_x = IP_x ML_x^{GS}$ and C_ϕ and CN_x are the covariance matrices of the layers modal turbulence and the noise of the WFS.

The P_x matrix computes the optimal DMs correction on selected optimizing directions extracted from the turbulence tomography. From Fusco^[10] and Le Roux^[11] P_x can be written in the DM modes space as:

$$P_x = \left[\frac{\sum_{i=1}^{N_Opt_x} \left[(MD_x^{Opt_i})^T MD_x^{Opt_i} \right]}{N_Opt_x} \right]^+ \left[\frac{\sum_{i=1}^{N_Opt_x} (MD_x^{Opt_i})^T ML_x^{Opt_i}}{N_Opt_x} \right]$$

Where $[]^+$ denotes the generalized inverse, N_Opt_x is the number of optimising directions, $MD_x^{Opt_i}$ is the matrix that project the DMs correction on the pupil in the selected optimization direction Opt_i and $ML_x^{Opt_i}$ is the matrix project the atmospheric wavefront distortions on the pupil in the selected optimization direction Opt_i . The matrix P is updated in soft real time (secondary loops).

The chosen coordinate system allows us to increase the updating period of the huge PR matrix of the HO loop to about 6 minutes, while the ones of the LO and REF loops are updated every about 15 seconds (they depends on the sky rotation with respect to the pupil). Moreover in the case of the HO loop the fitting projector P as well as the ML^{OPT} , that sums into the pupil the contribution of the different atmospheric layer in the directions of the guide stars, are pre-computed and retrieved from a database. In the case of LO and REF loops all the required matrices to get PR must be computed on line since the involved geometry is not fixed but it depends on positions of the NGS on sky.

In Figure 3 the parameters and computing power of the secondary loop are summarized.

	PR	R	$A = IP ML^{GS}$	IP	ML^{GS}	P	MD^{Opt_i}	ML^{Opt_i}	MD^{GS}	
	($Ncom, Nslp$)	($Nml \cdot Nl, Nslp$)	($Nslp, Nml \cdot Nl$)	($Nslp, Nwfs \cdot Nmp$)	($Nwfs \cdot Nmp, Nml \cdot Nl$)	($Ncom, Nml \cdot Nl$)	($Nmp, Ncom$)	($Nmp, Nml \cdot Nl$)	($ID=IP MD^{GS}, (Nwfs \cdot Nmp, Nslp, Ncom)Ncom$)	
TOTAL										
HO DATABASE										
Number of entries					1000	1000			1000	
N. Ele. (Gelements)					1500	310			357,12	
Single prec. (GB)	8668,48				6000	1240			1428,48	
updating period (s)					360	15			360	
Data rate(GB/s)	1,03E-01				1,67E-02	8,27E-02			3,97E-03	
COMPUTATIONS										
Operations	3,57E+13	1,01E+15	2,87E+13	Fixed	9,37E+15	7,56E+12	1,9375E+14	1,56E+15	2,142E+13	1,16E+15
Period (s)	360	360	360		360	15	15	15	360	360
Comp. power (GFlops)	2993	99	2814	80	26042	505	12917	104167	60	3229
REF COMPUTATIONS										
Operations	2,16E+09	2,68E+10		Fixed	1,20E+10	6,68E+08	6,00E+08	4,00E+09	6,47E+08	1,80E+09
Period (s)	15	15			15	15	15	15	15	15
Comp.g power (GFlops)	3,246	0,143	1,788		0,8	4,45E-02	0,04	0,266	4,32E-02	0,12
LO COMPUTATIONS										
Operations	1,05E+05	5,84E+07		Fixed	1,20E+06	1,59E+05	2,20E+04	4,00E+05	3,14E+04	6,60E+04
Period (s)	15	15			15	15	15	15	15	15
Comp. power (GFlops)	0,00402662	7,02E-06	3,89E-03		0,00008	1,06E-05	1,47E-06	2,66E-05	2,09E-06	0,0000044

Figure 3. Secondary loop parameters.

5. CONCLUSIONS

We have given in this paper a very fast overview of the MAORY Real Time Computer actual concept. The reconstruction is based on two POLC loops (HO and LO) which results are concatenated. A third slower POLC loop (REF) is devoted to offsets computation. The time filtering is applied directly to the commands. A smart coordinate system has been chosen in order to minimize the required computing power.

REFERENCES

- [1] Ciliegi, P. and others, "Maory for elt: preliminary design overview," in [Adaptive Optics Systems VI], Proc. SPIE 10703-38 (2018)
- [2] Tamai, R. and others, "The ESO's ELT construction status," in [Ground-based and Airborne Telescopes VII], Proc. SPIE 10700, 10700-36 (2018)
- [3] Davies, R. and others., "The MICADO first light imager for ELT: overview and operation," in [Ground-based and Airborne Instrumentation for Astronomy VII], Proc. SPIE 10702, 10702-64 (2018)
- [4] Clénet, Y. and others., "The MICADO first light imager for the ELT: towards the preliminary design review of the MICADO-MAORY SCAO," in [Adaptive Optics Systems VI], Proc. SPIE 10703, 10703-40 (2018).
- [5] Schreiber, L. and others., "The MAORY Laser Guide Star Wavefront Sensor: Design status," in [Adaptive Optics Systems VI], Proc. SPIE 10703, 10703-71 (2018)
- [6] Bonaglia, M. and others., "Status of the preliminary design of the ngs wfs subsystem of maory," in [Adaptive Optics Systems VI], Proc. SPIE 10703, 10703-164 (2018)
- [7] Rigaut, F. and Gendron, E., "Laser guide star in adaptive optics : the tilt determination problem," *Astron. Astrophys.* 261, 677-684 (1992)
- [8] Downing, M. and others., "Update on development of wfs cameras at ESO for the ELT," in [Adaptive Optics Systems VI], Proc. SPIE 10703, 10703-69 (2018)
- [9] Schreiber, L. and others., "Impact of sodium layer variations on the performance of the E-ELT MCAO module," Proc. SPIE 9148, 91486Q (2014)
- [10] Fusco, T. and others, "Optimal wave-front reconstruction strategies for multiconjugate adaptive optics," *J. Opt. Soc. Am. A*, Vol. 18 (2001)
- [11] Le Roux, B. and others, "Optimal control law for classical and multiconjugate adaptive optics," *J. Opt. Soc. Am. A*, Vol. 21, issue 7, pp. 1261-1276 (2004)